# Growth of Si and C $\delta$-doped *nipi* doping superlattices in GaAs by metal organic vapor phase epitaxy

G. Li[a] and C. Jagadish
*Department of Electronic Materials Engineering, The Research School of Physical Sciences and Engineering, The Institute of Advanced Studies, The Australian National University, Canberra ACT 0200, Australia*

M. B. Johnston and M. Gal
*School of Physics, The University of New South Wales, Sydney NSW 2052, Australia*

(Received 26 August 1996; accepted for publication 28 October 1996)

We have optimized growth conditions of metal organic vapor phase epitaxy (MOVPE) in order to grow Si and C $\delta$-doped *nipi* doping superlattices in GaAs. Trimethylaluminium (TMAl) and silane ($SiH_4$) were used as $p$-type and $n$-type doping precursors, respectively. We report that at 630 °C, full compensation of free electrons and holes can be obtained in the MOVPE-grown Si and C $\delta$-doped *nipi* doping superlattices over a very wide range of the sheet carrier densities ($10^{12}$–$10^{13}$ $cm^{-2}$) by choosing proper TMAl flow rate and Si $\delta$-doping time or $SiH_4$ flow rate. The experimental results on electrical and optical characterization of Si and C $\delta$-doped *nipi* doping superlattices in GaAs with 150 Å thick undoped spacer layers are presented. © *1996 American Institute of Physics.* [S0003-6951(96)03253-6]

During the last decade, unique charge transport-assisted optical and electrooptic nonlinear properties of *nipi* doping superlattices have been extensively investigated.[1–4] A number of novel devices based on *nipi*s have been demonstrated.[5–8] The inherently random impurity distribution in doped layers can produce potential fluctuations which may be sufficiently large to diminish effects arising from the modulation of the bulk energy bands.[9] This potential fluctuation can be greatly reduced in the growth direction by incorporating $\delta$-function-like doped layers.[10,11] Recently, theoretical calculations predicted that strategic $\delta$-doping can significantly improve low voltage operation of modulators.[12] Hence growth of $\delta$-doped *nipi* doping superlattices is of great interest not only to fundamental studies but also to exploitation of new device structures. For non-linear optical and electro-optic applications, full compensation of $n$-type and $p$-type carriers in $\delta$-doped *nipi* doping superlattices is crucial.

In molecular beam epitaxy (MBE), the sheet $\delta$-doping concentration can be accurately controlled by the product of the dopant exposure time and dopant cell temperature. The dopant segregation can be effectively eliminated by using low growth temperatures ($<600$ °C).[11] The success in the MBE-growth of Si and Be $\delta$-doped GaAs has led to fabrication of a variety of $\delta$-doped *nipi* structures.[6–8,10,11] Recently, high quality Si, Zn and C $\delta$-doped GaAs have been successfully grown by metal organic vapor phase epitaxy (MOVPE).[13–15] To the best of our knowledge, however, there has been no report on growth of $\delta$-doped *nipi* in GaAs. The major difficulties encountered for MOVPE to grow $\delta$-doped *nipi* structures include the complicated dopant incorporation mechanism and the distinct temperature dependence of $n$-type and $p$-type doping concentration.[13,14]

The most widely used dopants in MOVPE are Si for $n$-type and Zn or C for $p$-type $\delta$-doping. It is well known that the Si doping concentration significantly increases but the Zn or C doping concentration substantially decreases with an increase in growth temperature. As a result, it becomes extremely difficult to find one growth temperature, at which the same $n$-type and $p$-type $\delta$-doping concentration can be achieved for the full compensation. In this work, the Si and C $\delta$-doped *nipi* in GaAs were grown in MOVPE. We report that the full compensation of free electrons and holes, generated from Si and C $\delta$-doped layers, respectively, can be achieved by optimizing the Si and C $\delta$-doping parameters at one growth temperature of 630 °C. The background concentration of free carriers and optical properties of the Si and C $\delta$-doped *nipi* were characterized by the electrochemical capacitance-voltage profiling and low temperature photoluminescence measurements.

The growth precursors were trimethylgallium (TMGa) and 100% $AsH_3$. The doping precursors were trimethylaluminium (TMAl) and 500 ppm $SiH_4$ diluted in hydrogen. The reactor pressure and $H_2$ carrier gas flow rate were 76 Torr and 17.5 slm. During the Si $\delta$-doping step, the reactor pressure and $H_2$ carrier gas flow rate were changed to 400 Torr and 2 slm in order to increase the Si doping efficiency.[13] Growth rate of GaAs was 2.6 $\mu$m/h with a constant V/III ratio of 200. Epi-ready semi-insulating and $n^+$ $\langle 100 \rangle$ GaAs wafers oriented 2° off towards (110) were used as substrates. The detailed $\delta$-doping sequence was described in our previous articles.[13,15] Briefly, the pre-$\delta$-doping purge time was 10 s for C $\delta$-doping and 8 s for Si $\delta$-doping both with an $AsH_3$ flow rate of 15 sccm. The $\delta$-doping time was 4 s for C $\delta$-doping without any $AsH_3$ and variable for Si $\delta$-doping with an $AsH_3$ flow rate of 160 sccm. No post-$\delta$-doping purge step in Si $\delta$-doping but 4 s post-$\delta$-doping purge step for C $\delta$-doping with an $AsH_3$ flow rate of 35 sccm was employed. The carrier profiles of the doping superlattices were obtained using a BIO-RAD 4300 electrochemical capacitance-voltage profiler (EC-V). The electrolyte was a NaOH:EDTA solution.

[a]Electronic mail: gli109@rsphy6.anu.edu.au

 0003-6951/96/69(27)/4218/3/$10.00 © 1996 American Institute of Physics

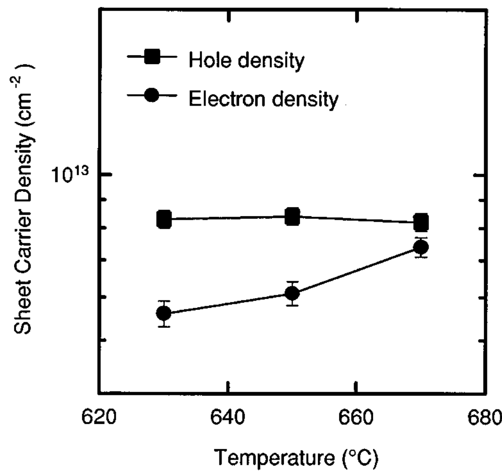


FIG. 1. Temperature dependence of the sheet hole and electron density of C and Si $\delta$-doped GaAs. Si $\delta$-doping time was 40 s. The flow rates of TMAl and $SiH_4$ were $6.35\times10^{-6}$ and $4.35\times10^{-7}$ mol/min, respectively.

The hole and electron density of C and Si $\delta$-doped GaAs as a function of growth temperature are shown in Fig. 1. Over the experimental range of 630–670 °C, the electron density is lower than the hole density under our growth conditions. The C $\delta$-doping is implemented by the deposition of a small amount of the TMAl on the nongrowing GaAs surface in the $AsH_3$ free ambient. The thermally decomposed Al-$(CH_3)_x$ species are the responsible doping species. Compared to the other C $\delta$-doping precursor,[16] the strong bonding of $AlCH_3$ (65 kcal/mol) eventually leads to less temperature dependence of the free hole density. By comparison, Si $\delta$-doping concentration is controlled by thermally activated reactions taking place in the gas phase.[13,17] Even though the change of the growth temperature is very small (for example, changed by 40 °C in Fig. 1), its effect on the electron density is quite significant. As a result, the gap between the hole and electron density widens as the temperature is reduced. At the highest growth temperature used in Fig. 1, the electron density approximates the hole density. But on the other hand, a low growth temperature is always highly desired in order to minimise the *in situ* thermal diffusion of the dopants. Thus, the same electron and hole density of Si and C $\delta$-doped layers is better to be achieved by using proper values of other growth parameters at the lowest possible growth temperature.

For C $\delta$-doping, either the TMAl flow rate or $\delta$-doping time could be varied for different doping concentrations. We found that an extended $\delta$-doping time may seriously degrade morphology since in the duration of $\delta$-doping, there is no $AsH_3$ overpressure. The hole density was therefore altered by changing the TMAl flow rate. The previous study shows that a number of $\delta$-doping parameters affect Si $\delta$-doping concentration.[13,17] Among those parameters, the $\delta$-doping time and $SiH_4$ flow rate are the best variable parameters in terms of their capability to effectively change the electron density. Hence, the variation of the electron density was obtained by either changing Si $\delta$-doping times at the fixed $SiH_4$ flow rate or altering $SiH_4$ flow rate at the given $\delta$-doping time of 30 s.

It can be seen in Fig. 2 that the hole and electron density

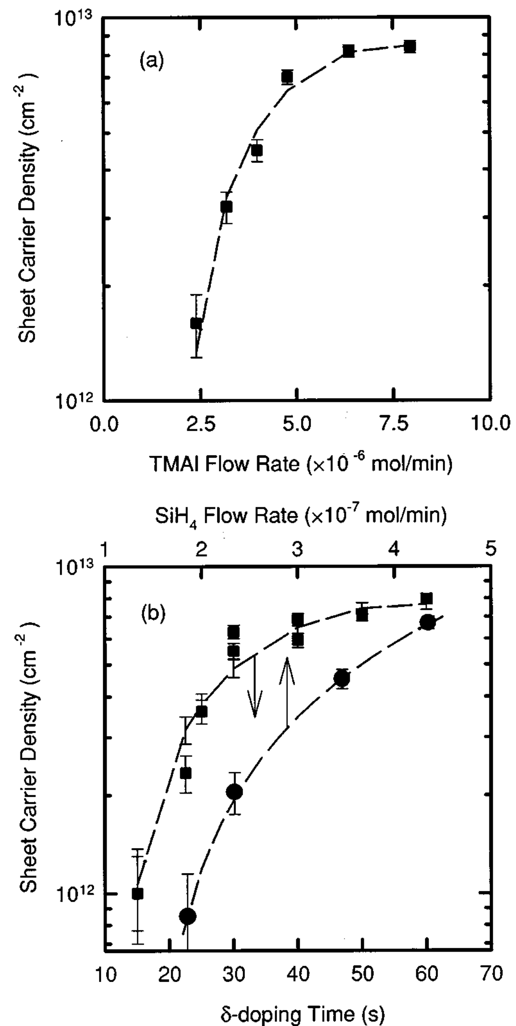


FIG. 2. Dependencies of the sheet hole density of C $\delta$-doped GaAs on TMAl flow rate (a) and the sheet electron density of Si $\delta$-doped GaAs on $\delta$-doping time at the given $SiH_4$ flow rate of $4.35\times10^{-7}$ mol/min or $SiH_4$ flow rate at the given $\delta$-doping time of 30 s (b).

both vary from $\sim 10^{12}$ to $\sim 10^{13}$ cm$^{-2}$ over the experimental regions of the TMAl flow rate and Si $\delta$-doping time or $SiH_4$ flow rate. Based on Fig. 2, the proper growth parameters for Si and C $\delta$-doping can be chosen to obtain the fully compensated Si and C $\delta$-doped *nipi* in GaAs. For example, in order to fabricate Si and C $\delta$-doped *nipi*, in which the sheet carrier concentration of Si and C $\delta$-doped layers was $3.2\times10^{12}$ cm$^{-2}$, the TMAl flow rate of $3.18\times10^{-6}$ mol/min and the Si $\delta$-doping time of 22.5 s at the $SiH_4$ flow rate of $4.35\times10^{-7}$ mol/min are recommended. Figure 2 also indicates that simply by changing the TMAl flow rate and the $SiH_4$ flow rate or $\delta$-doping time at 630 °C, the electron and hole density respectively vary by almost over one order of magnitude. This gives great flexibility to design Si and C $\delta$-doped *nipi* having different sheet densities.

The Al incorporation along with the C during the $\delta$-doping was confirmed by the Al profiling carried out with the secondary ion mass spectroscopy (SIMS). The SIMS spectra qualitatively show that only a very small amount of the Al atoms are incorporated even when using the highest TMAl flow rate [see Fig. 2(a)]. If there was a considerable amount of the Al incorporated during the $\delta$-doping, an Al-

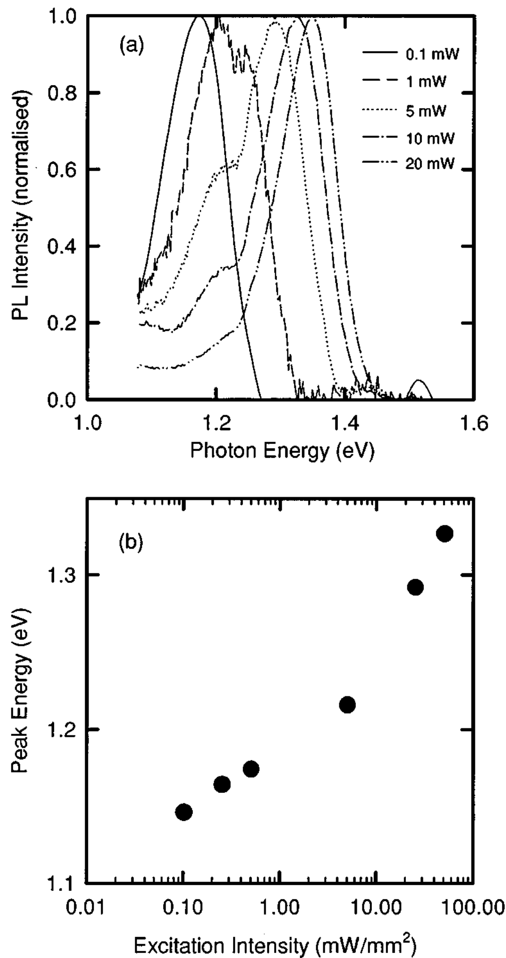


FIG. 3. Variation of photoluminescence (PL) with photoexcitation power (laser beam diameter was 0.5 mm) at 12 K (a) [ the spectrum obtained using the lowest intensity was curve-smoothed], and the PL peak energy as a function of photoexcitation intensity (b). Si and C $\delta$-doped *nipi* doping superlattice has 150 Å undoped spacer layer between Si and C $\delta$-doped layers. The growth temperature was 630 °C. Si $\delta$-doping time was 22.5 s with the $SiH_4$ flow rate of $4.35\times10^{-7}$ mol/min. The TMAl flow rate was $3.18\times10^{-6}$ mol/min.

rich layer would be formed at the position of the $\delta$-doped layer. Consequently, this should lead to corresponding photoluminescence (PL). The detailed study of low temperature PL shows that this Al incorporation does not affect optical properties of the Si and C $\delta$-doped *nipi* doping superlattices with the undoped spacer layer thickness between 100 and 300 Å.

The Si and C $\delta$-doped *nipi*, in which the sheet carrier density of the Si and C $\delta$-doped layers was $3.2\times10^{12}$ $cm^{-2}$ and the undoped spacer layer thickness between two neighbouring $\delta$-doped layers was 100– 300 Å, were grown for electrical and optical characterisation. The EC-V measurements show that the background of those doping superlattices is $n$-type with the electron density of $<2\times10^{16}$ $cm^{-3}$. This residual electron density is comparable to the background concentration ($\sim3\times10^{16}$ $cm^{-3}$) of undoped GaAs. The carrier profile, measured by the conventional capacitance-voltage profiling, of single Si or C $\delta$-doped layer in GaAs, has the peak density of $\sim3\times10^{18}$ $cm^{-3}$ with a full width at half maximum of 50–60 Å. Apparently, in terms of free electron and hole density, the Si and C $\delta$-doped doping superlattices have been well compensated.

The variation of PL with photoexcitation intensity is one of the unique characteristics of doping superlattices.[18,19] The PL spectra as a function of photoexcitation intensity is illustrated in Fig. 3(a). The asymmetric PL line shape, with a steep high energy edge and a trailing tail on the low energy side, is similar to that observed in bulk-doped doping superlattices[18] and MBE grown Si and Be $\delta$-doped doping superlattices.[10,11] Figure 3(b) shows the PL peak energy as a function of photoexcitation intensity. The PL peak energy shifts to higher energy with increasing excitation intensity due to screening of the superlattice potential by photogenerated carriers. Over the experimental range of excitation intensity, the peak energy shifts by about $\sim$200 meV. These optical results further confirm that the full compensation of free electrons and holes has been achieved in our Si and C $\delta$-doped doping superlattices.

In conclusion, the fully compensated Si and C $\delta$-doped *nipi* doping superlattices in GaAs have been successfully grown for the first time in MOVPE. The sheet carrier concentration of Si and C $\delta$-doped layers over the region of $\sim10^{12}$ to $\sim10^{13}$ $cm^{-2}$ can be obtained simply by changing the TMAl flow rate and Si $\delta$-doping time or $SiH_4$ flow rate at 630 °C. The background carrier concentration of the Si and C $\delta$-doped *nipi* is $<2\times10^{16}$ $cm^{-3}$ which is about 2 orders of magnitude lower than the peak carrier concentration ($\sim3\times10^{18}$ $cm^{-3}$) of single Si and C $\delta$-doped layers. Significant variation of PL peak wavelength with photoexcitation intensity was also observed. Over the intensity range of 0.1–100 (mW $mm^{-2}$), the PL peak energy shifts by about 200 meV.

The authors wish to acknowledge financial support of the Australian Research Council (ARC).


[1] G. H. Döhler, Opt. Quantum Electron. **<dbxNULL>22**, S121 (1990).
[2] G. H. Döhler, Superlattices Microstruct. **8**, 49 (1990).
[3] M. K. Hibbs-Brenner, P. P. Ruden, J. A. Lehman, J. J. Liu, and R. A. Walterson, IEEE J. Quantum Electron. **30**, 1227 (1994).
[4] P. J. Poole, C. C. Phillips, C. Rorts, and M. Paxman, IEEE J. Quantum Electron. **30**, 1027 (1994).
[5] X. Leijtens, G. W. Yoffe, J. E. M. Haverkort, F. Karouta, J. Brubach, T. Eijkemans, L. M. F. Kaufmann, M. K. Smit, J. A. A. Stegemann, Y. C. Zhu, and J. H. Wolter, Appl. Phys. Lett. **66**, 2736, (1995).
[6] A. G. Larsson and J. Maserjian, Opt. Eng. **31**, 1576 (1992).
[7] S. D. Koehler, E. M. Garmire, A. R. Kost, D. Yap, D. P. Docter, and T. C. Hasenberg, IEEE Photonics Technol. Lett. **7**, 878 (1995).
[8] G. W. Yoffe, J. Brüback, F. Karouta, W. C. van der Vleuten, L. M. F. Kaufmann, and J. H. Wolter, Appl. Phys. Lett. **63**, 1456, (1993).
[9] P. Ruden and G. H. Döhler, Phys. Rev. B **27**, 3538 (1983).
[10] E. F. Schubert, T. D. Harris, and J. E. Cunningham, Appl. Phys. Lett. **53**, 2208 (1988).
[11] E. F. Schubert, *Semiconductors and Semimetals*, edited by A. C. Gossard (Academic, New York), Vol. 40, p. 1.
[12] W. Batty and D. W. E. Allsopp, IEEE Photonics Technol. Lett. **7**, 635 (1995).
[13] G. Li and C. Jagadish, J. Cryst. Growth **167**, 421 (1996).
[14] G. Li, M. Linnarsson, and C. Jagadish, J. Cryst. Growth **154**, 231 (1995).
[15] G. Li, M. Petravic, and C. Jagadish, J. Appl. Phys. **79**, 3554 (1996).
[16] T. Makimoto and N. Kobayashi, Jpn. J. Appl. Phys. **32**, L1300 (1993).
[17] G. Li and C. Jagadish, Mater. Sci. Eng. B **33**, 182 (1995).
[18] G. H. Döhler, H. Kunzei, D. Olego, K. Ploog, P. Ruden, H. J. Stolz, and G. Abstreiter, Phys. Rev. Lett. **47**, 864 (1981).
[19] A. P. Thorn, P. C. Klipstein, and R. W. Glew, IEE Proc. J. **136**, 38 (1989).